

RESEARCH

Open Access



Transcriptional insights into *Chlorella* sp. ABC-001: a comparative study of carbon fixation and lipid synthesis under different CO₂ conditions

Hyun Gi Koh¹, Jun Muk Cho², Seungjib Jeon², Yong Keun Chang², Bongsoo Lee^{3*} and Nam Kyu Kang^{4*}

Abstract

Background Microalgae's low tolerance to high CO₂ concentrations presents a significant challenge for its industrial application, especially when considering the utilization of industrial exhaust gas streams with high CO₂ content—an economically and environmentally attractive option. Therefore, the objectives of this study were to investigate the metabolic changes in carbon fixation and lipid accumulation of microalgae under ambient air and high CO₂ conditions, deepen our understanding of the molecular mechanisms driving these processes, and identify potential target genes for metabolic engineering in microalgae. To accomplish these goals, we conducted a transcriptomic analysis of the high CO₂-tolerant strain, *Chlorella* sp. ABC-001, under two different carbon dioxide levels (ambient air and 10% CO₂) and at various growth phases.

Results Cells cultivated with 10% CO₂ exhibited significantly better growth and lipid accumulation rates, achieving up to 2.5-fold higher cell density and twice the lipid content by day 7. To understand the relationship between CO₂ concentrations and phenotypes, transcriptomic analysis was conducted across different CO₂ conditions and growth phases. According to the analysis of differentially expressed genes and gene ontology, *Chlorella* sp. ABC-001 exhibited the development of chloroplast organelles during the early exponential phase under high CO₂ conditions, resulting in improved CO₂ fixation and enhanced photosynthesis. Cobalamin-independent methionine synthase expression was also significantly elevated during the early growth stage, likely contributing to the methionine supply required for various metabolic activities and active proliferation. Conversely, the cells showed sustained repression of carbonic anhydrase and ferredoxin hydrogenase, involved in the carbon concentrating mechanism, throughout the cultivation period under high CO₂ conditions. This study also delved into the transcriptomic profiles in the Calvin cycle, nitrogen reductase, and lipid synthesis. Particularly, *Chlorella* sp. ABC-001 showed high expression levels of genes involved in lipid synthesis, such as glycerol-3-phosphate dehydrogenase and phospholipid-diacylglycerol acyltransferase. These findings suggest potential targets for metabolic engineering aimed at enhancing lipid production in microalgae.

Conclusions We expect that our findings will help understand the carbon concentrating mechanism, photosynthesis, nitrogen assimilation, and lipid accumulation metabolisms of green algae according to CO₂ concentrations.

*Correspondence:

Bongsoo Lee
bongsoolee@mokwon.ac.kr
Nam Kyu Kang
nkkang@khu.ac.kr

Full list of author information is available at the end of the article



© The Author(s) 2023. **Open Access** This article is licensed under a Creative Commons Attribution 4.0 International License, which permits use, sharing, adaptation, distribution and reproduction in any medium or format, as long as you give appropriate credit to the original author(s) and the source, provide a link to the Creative Commons licence, and indicate if changes were made. The images or other third party material in this article are included in the article's Creative Commons licence, unless indicated otherwise in a credit line to the material. If material is not included in the article's Creative Commons licence and your intended use is not permitted by statutory regulation or exceeds the permitted use, you will need to obtain permission directly from the copyright holder. To view a copy of this licence, visit <http://creativecommons.org/licenses/by/4.0/>. The Creative Commons Public Domain Dedication waiver (<http://creativecommons.org/publicdomain/zero/1.0/>) applies to the data made available in this article, unless otherwise stated in a credit line to the data.

This study also provides insights into systems metabolic engineering of microalgae for improved performance in the future.

Keywords Microalgae, *Chlorella*, Transcriptomic analysis, CO₂ fixation, Lipid accumulation

Background

Due to the massive use of fossil fuels and deforestation, the carbon dioxide in the atmosphere is continuously increasing, causing global warming. Hence, the demand for sustainable alternative energy is promoting research on microalgae because of their potential for CO₂ reduction and biofuel production. Microalgae are known to have much higher photosynthetic efficiency as compared to terrestrial plants [1, 2]. Indeed, around 27,200 tons of CO₂ are commercially converted into microalgal biomass annually [3–5]. As such, microalgae are considered to be one of the best candidates for CO₂ sequestration [6]. However, microalgae's low tolerance to high CO₂ concentrations poses a significant challenge to its commercialization [7]. This is especially important when considering the utilization of industrial exhaust gas streams with high CO₂ content (>10%), which is the most economical and environmentally attractive option [8–11].

Chlorella sp. is one of the most studied microalgae for lipid and CO₂ sequestration [12, 13]. A whole genome sequence has been unveiled in several *Chlorella* sp., and diverse genetic manipulation tools, including CRISPR/Cas9 and transformation methods, have been developed [14–16]. Recently, multiple transcriptomic analyses have been carried out under diverse conditions to understand the mechanisms of CO₂ fixation, lipid accumulation, and stress resistance in *Chlorella* sp. (Table 1) [13, 17–28]. In particular, research has been conducted on the photosynthesis of these strains under high CO₂ concentrations, as *Chlorella* is known to have strains that have a tolerance to high CO₂ compared to other species [13, 22, 28–30].

Photosynthesis with CO₂ fixation is one of the most crucial bioprocesses in microalgae. Photosynthetic efficiency is highly affected by the concentration of the dissolved CO₂ in a media. Huang et al. estimated the K_m value of RuBisCo (Ribulose-1,5-bisphosphate carboxylase) in *Chlorella* PY-ZU1 to be in the range of 80–192 μM, which exceeds the dissolved CO₂ concentration (~15 μM) in water with air at an equilibrium state, indicating the necessity of CO₂ concentrating mechanism (CCM) in microalgae [13, 31]. Carbonic anhydrase (CA) is the key enzyme for CCM, as it converts CO₂ into more soluble HCO₃⁻, allowing the dissipation of HCO₃⁻ into the cell. Then, CA helps CO₂ fixation by reconvert-ing the internalized HCO₃⁻ into CO₂ at the thylakoid membrane under low CO₂ concentrations. Hence, CA is highly expressed under CO₂-limited conditions along

with other CCM-related enzymes. Additionally, Jianhua et al. proposed several transporters related to CCM, which showed significant expression changes in the short term (0–24 h) by CO₂ deprivation in *Chlorella pyrenoidosa* [21]. Besides, the previous transcriptomic profile of *C. pyrenoidosa* has also revealed 8 unigenes including ABC transporter, chlorophyll a/b binding protein, and photosystem I subunit V, which may play essential roles in CCM as well [20]. Although these findings have provided some information about CCM in *Chlorella* sp., there are still many unknown points underlying the CCM mechanisms.

The lipid accumulation mechanism in microalgae has been investigated over the years as lipids could be converted into biofuels or purified for human consumption (e.g. cooking oils, polyunsaturated fatty acids). In general, lipid production occurs primarily in the endoplasmic reticulum (ER) or chloroplast through the Kennedy pathway, storing energy in the form of triacylglycerol (TAG). Hence, many approaches for overexpression of Kennedy pathway genes including *glycerol-3-phosphate dehydrogenase (GPDH)*, *glycerol-3-phosphate acyltransferase (GPAT)*, *lysophosphatidic acid acyltransferase (LPAT)*, *phosphatidic acid phosphohydrolase (PAP)*, and *diacylglycerol acyltransferase (DGAT)* has been reported, especially in oleaginous algae species such as *Phaeodactylum* and *Nannochloropsis* [32–34]. The lipid accumulation pathway in *Chlorella* sp. has also been extensively studied at the transcriptome level under various stress conditions [18, 35–37].

Most microalgal CO₂ conversion studies have been conducted under moderately high CO₂ conditions of 5% or below, and microalgae that grow well under 5–20% CO₂ are considered CO₂-tolerant strains [40]. *Chlorella* sp. ABC-001 showed enhanced growth under 10–15% CO₂ conditions as compared to ambient air conditions [38, 39]. Thus, it is necessary to understand insights into the response of CO₂-tolerant strain under high CO₂ conditions for the use of industrial flue gases. Additionally, most studies focusing on lipid synthesis and transcriptomic analysis manipulate media composition or impose artificial stress to observe short-term changes. However, in large-scale cultivation, applying artificial stress is complex. This highlights the significance of studying natural nutrient depletion, an aspect that has received comparatively less attention in the field. Accordingly, it is meaningful to study the relationships between phenotypes and

Table 1 Transcriptomic studies conducted in *Chlorella* sp.

Species	Habitat	Purpose of transcriptomics	Variables	Lipid Analysis	Carbon source	Analyzed samples	Ref.
<i>Chlorella pyrenoidosa</i> FACHB-9	Freshwater	Redirection of central metabolism when CO ₂ is deprived	Growth after CO ₂ stress	n.a	5% CO ₂ → AA	0 h, 1 h, 4 h, 24 h	[21]
<i>Chlorella pyrenoidosa</i> 820	Marine	Transcriptomic changes on different CO ₂ conditions	CO ₂	n.a	0.16% CO ₂ 0.04% CO ₂	Day 2, 0.16% CO ₂ Day 2, 0.04% CO ₂	[20]
<i>Chlorella</i> PY-ZU1	Freshwater	Carbon fixation mechanism of high CO ₂ -tolerant <i>Chlorella</i>	Growth phase CO ₂	n.a	15% CO ₂ Ambient air	12 h, 24 h, 48 h, 72 h 15% CO ₂ 12 h, 24 h, 48 h, 72 h Ambient air	[13]
<i>Chlorella</i> sp. ABC-001	Marine	Growth specific changes in carbon fixation and lipid accumulation at high CO ₂ condition	Growth phase CO ₂	Total fatty acids by GC	10% CO ₂ Ambient air	Day 1, 3, 7, 10% CO ₂ Day 1, 3, 7, Ambient air	[This study]
<i>Chlorella zofingiensis</i> ATCC 30412	Freshwater	To identify genes and their expression level involved in astaxanthin and TAG biosynthesis	Carbon source	Total fatty acids by GC	Ambient air Glucose (glc)	6 h	[19]
<i>Chlorella vulgaris</i> UPSI-JRM01	Freshwater	Carbon partitioning toward starch and TAGs under nitrogen stress	Growth after nitrogen stress	Total fatty acids by GC	5% CO ₂	Day 1, 4, 8	[18]
<i>Chlorella pyrenoidosa</i> FACHB-10	Freshwater	To affirm the role of lipid turnover and identify differentially expressed transcription factors under nitrogen deprivation	Nitrogen	Fatty acids by GC-MS Lipid analysis by HPLC-MS	Ambient air	Day 2, 1.5 g/L nitrate Day 2, 0 g/L nitrate	[23]
<i>Chlorella</i> sp. C596	Marine	Transcriptomic changes before and after nutrient (nitrogen) deprivation	Nitrogen	TAGs by HPLC	15% CO ₂ for pH control	109 h, 192 h	[22]
<i>Chlorella sorokiniana</i> G32	Freshwater	To explain high starch accumulation and growth rate under mixotrophic condition	Glucose	Total lipid by gravimetric method	1.25 g/L glc 5 g/L glc	Before & After 1.25 g/L → 5 g/L glc Before & After 5 g/L → 1.25 g/L glc	[24]
<i>Chlorella</i> sp. TLD68	Freshwater	To clarify the relationship between salt tolerance and lipid accumulation	Salt stress	Sulfo-phospho-vanillin fluorescence	Ambient air	18 h, 0 M NaCl 18 h, 0.1 M NaCl 18 h, 0.8 M NaCl	[25]
<i>Chlorella sorokiniana</i> UTEX 1602	Freshwater	DEGs in photosynthetic carbon fixation and lipid production under different nitrogen conditions and carbon source	Nitrogen Carbon source	Nile-red fluorescence	4% glc 4% CO ₂	48 h, 0.2% nitrate 48 h, 0.8% nitrate 84 h, 0.2% nitrate, heterotrophic Day 8 0.033% nitrate, 4% CO ₂	[17]

Table 1 (continued)

Species	Habitat	Purpose of transcriptomics	Variables	Lipid Analysis	Carbon source	Analyzed samples	Ref.
<i>Chlorella</i> sp. BLD	Freshwater	Mechanisms of alkali resistance and lipid accumulation in the alkaliphilic microalgae <i>Chlorella</i> sp. BLD	pH	Total lipid by gravimetric method	Ambient air	Day 2 pH 10 Day 2 pH 7.5	[36]
<i>Chlorella</i> sp. UMACC 237	Freshwater	Compare transcriptome profile of at ambient (4 °C) versus stress-inducing high (33 °C) temperatures	Temperature	n.a	Ambient air	120 h 4°C 120 h 33°C	[26]
<i>Chlorella sorokiniana</i> NIES-2168	Freshwater	To elucidate the effects of glucose assimilation and light intensity	Carbon source	n.a	Ambient air 2% glucose	Day 7 Autotrophic Day 7 Mixotrophic	[35]
<i>Chlorella vulgaris</i> PKVL 7422	Freshwater	To elucidate the effect of salt stress on metabolism and possible mechanisms of survival	Salt stress	n.a	Ambient air	Control without salt stress 2 h, 4 h NaCl 1% 2 h, 4 h NaCl 3%	[37]
<i>Chlorella</i> sp. L5	Freshwater	Revealing the phenol tolerance mechanism	Evolved strain for phenol	n.a	TAP	Day 4, L5 strain Day 4, L3 strain	[49]
<i>Chlorella pyrenoidosa</i> FACHB-5	Freshwater	Transcriptomic and Physiological Responses during Exposure to 17 α -Ethinylestradiol	17 α -Ethinylestradiol (17 α EE ₂)	n.a	Ambient air	96 h 0 mg/L 17 α EE ₂ 96 h 2 mg/L 17 α EE ₂ 96 h 4 mg/L 17 α EE ₂ 96 h 8 mg/L 17 α EE ₂	[27]
<i>Chlorella</i> sp. Cv	Freshwater	To understand global response and possible tolerance mechanism against flue gas in an evolved strain	Flue gas	n.a	10% CO ₂	Day 1 flue gas Day 1 10% CO ₂	[28]

transcriptomic analysis according to CO₂ and nutrient concentrations.

In this study, we conducted a time-course transcriptomic analysis of *Chlorella* sp. ABC-001, the high-CO₂ tolerant strain, under ambient air and 10% CO₂ conditions. We analyzed transcriptomic changes related to CO₂ concentrations, cell growth phases, lipid accumulation, and nutrient depletion with a macroscopic perspective. Furthermore, we identified critical genes related to each metabolism and discussed them in detail. These findings are expected to enhance our understanding of the photosynthesis and lipid accumulation metabolism in the green alga *Chlorella* sp., especially under high CO₂ conditions. Our study will also provide valuable insights into the metabolic engineering and synthetic biology of microalgae.

Results

Cultivation of *Chlorella* sp. ABC-001 under ambient air and 10% CO₂ conditions

In this study, triplicate biological cultivations of *Chlorella* sp. ABC-001 were carried out in different CO₂ concentrations using photobioreactors for transcriptomic analysis. As described in Fig. 1, an apparent difference in growth and lipid accumulation was observed under the 10% CO₂ condition compared to the ambient air condition. The maximum growth rate was faster with CO₂ ($\mu_{\max}^{\text{CO}_2}$: 0.84 d⁻¹, μ_{\max}^{Air} : 0.72 d⁻¹), and the cells grew up to 2.5-fold higher cell density, accumulating almost twice more lipids (Fig. 1a, b). The nutrients were depleted faster in CO₂ conditions, which was consistent with faster cell growth (Fig. 1c). Nitrogen and sulfur were almost depleted on day 3 and day 4 at 10% CO₂, respectively,

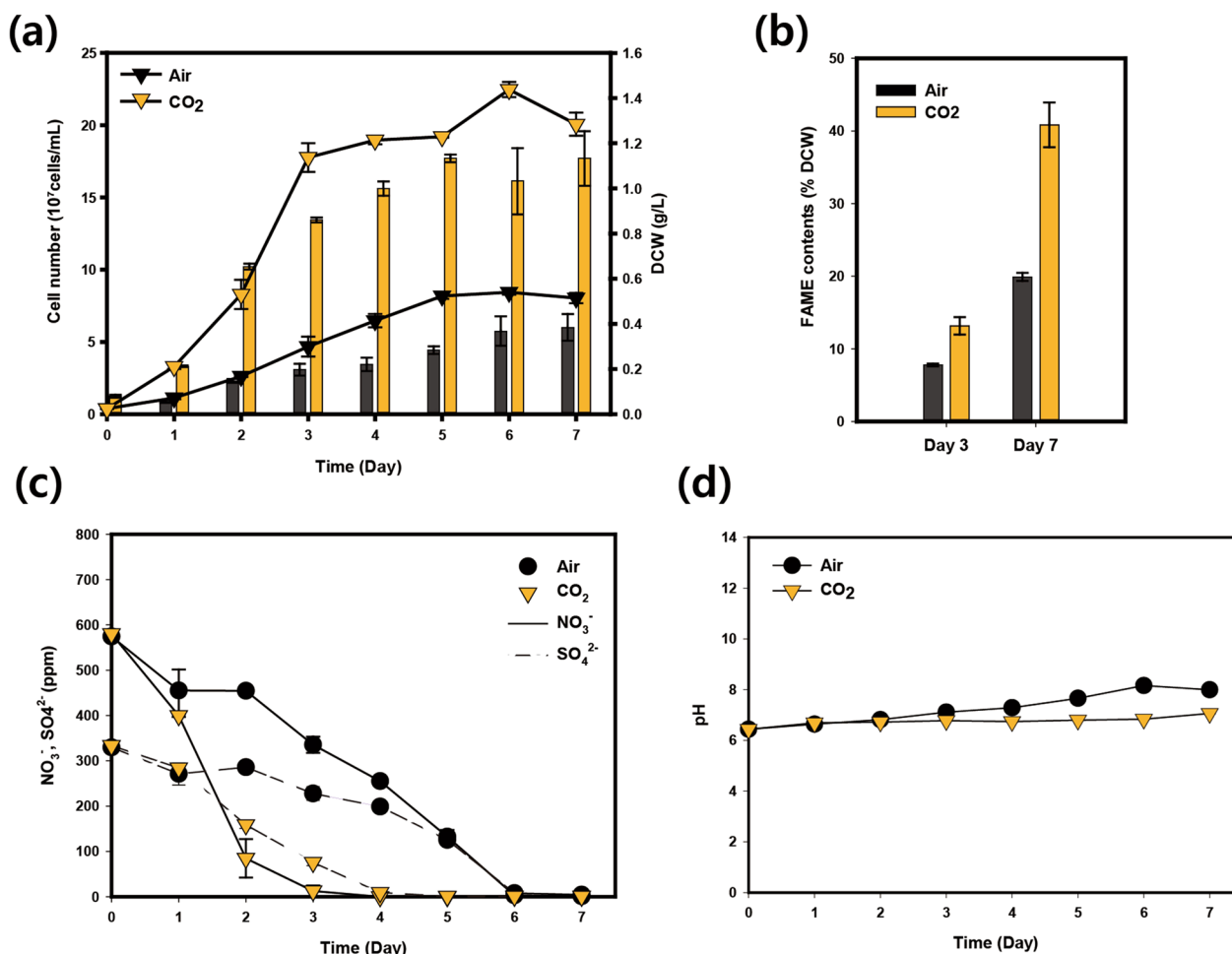


Fig. 1 Cultivation of *Chlorella* sp. ABC-001 under different CO₂ conditions. **a** Growth curve of cells cultivated with ambient air and 10% CO₂. The line graph represents cellular density, and the bar graph represents dried cell weight. **b** The lipid contents of cells as measured after transesterification into FAME. **c** Changes in nitrate concentration (NO₃⁻) and sulfate concentration (SO₄²⁻). **d** pH changes. Error bars stand for the standard error calculated from three independent experimental data sets. Asterisks indicate the significant difference between cells cultivated under ambient air and 10% CO₂ determined by Student's *t*-test (**P* < 0.05, ***P* < 0.01, ****P* < 0.001)

while it took 6 days to consume all these nutrients under ambient air conditions. The pH was maintained between 6 and 8 during the whole cultivation in both conditions, indicating that the effects of pH change may be negligible (Fig. 1d). Transcriptomic analysis through RNA sequencing was conducted to unravel the governing mechanisms and discover critical genes causing the phenotypic changes under different CO₂ concentrations.

RNA-sequencing and unigene assembly

The RNA samples were collected on days 1, 3, and 7 to represent the early-exponential phase, mid-exponential phase, and stationary phase under both ambient air and high CO₂ conditions. For simplification, cells collected from each condition will be represented by ‘A1, A3, A7’ and ‘C1, C3, C7’ (A: ambient air, C: 10% CO₂, 1: day1, 3: day3, 7: day7). The total number of 10–16 million (M) raw reads from the ambient air and high CO₂ samples were sequenced, and 8–14 M clean reads were generated after trimming and sorting, as described in the material and method section. The clean read ratio of the raw sequence was about 87.75%, and the pairs plot analysis showed that the reproducibility of biological triplicate samples was higher than 0.9 in most cases, ensuring high reproducibility and reliability of the data (Additional file 1: Fig. S1). Clean reads were pooled for assembly, and a total of 10,246 annotated unigenes were generated, as summarized in Additional file 1: Table S1. The top 3 species represented in the National Center for

Biotechnology Information (NCBI) non-redundant (NR) database were *Auxenochlorella protothecoides*, *Chlorella variabilis*, and *Coccomyxa subellipsoidea*, accounting for 52.7% of the transcripts (Additional file 1: Fig. S2). The whole transcriptomic data obtained in this study were deposited in the NCBI database under BioProject accession number PRJNA757763.

Analysis of differentially expressed genes across different growth phases and CO₂ concentrations

Pairwise transcriptome comparison was performed to identify differentially expressed genes (DEGs). We compared expression levels under high CO₂ conditions based on those under ambient air conditions on days 1, 3, and 7 (C1A: C1 vs A1, C3A: C3 vs A3, C7A: C7 vs A7). Basically, downregulated DEGs were more dominant than upregulated DEGs in all three comparisons under high CO₂ conditions, and the number of downregulated DEGs also increased as the cultivation progressed (Fig. 2a).

Among all the identified DEGs, only one gene, carbamoyl phosphate synthetase B (Csorokiniana-1SL000732t0001), showed a consistent upregulation in 10% CO₂ during the whole cultivation period (Fig. 2b). Carbamoyl phosphate synthetase participates in the nitrogen metabolism pathway, catalyzing the first committed step in pyrimidine and arginine production [41]. Thus, we assume that the high expression level of carbamoyl phosphate synthetase was due to the faster nitrogen uptake in high CO₂ conditions. The

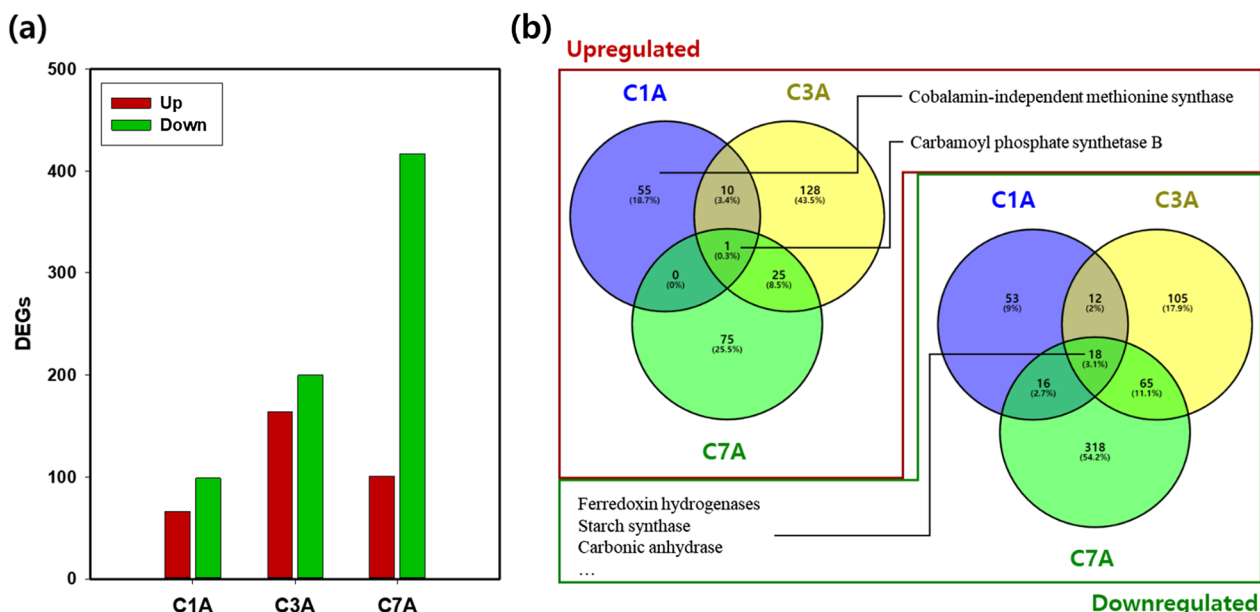


Fig. 2 Transcript profiling changes by CO₂ concentration. **a** The numbers of upregulated and downregulated DEGs in each condition. **b** Venn diagram representing the number of non-redundant DEGs from different CO₂ concentrations. The left and right Venn diagram each represents upregulated and downregulated DEGs. C1A, C3A, and C7A represent the DEGs comparison of C1 vs A1, C3 vs A3 and C7 vs A7, respectively

most notable upregulated gene was the cobalamin-independent methionine synthase (METE, Csorokina1SL000035t0006), which was observed in the C1A comparison. The expression level of METE was 20–32 fold higher in the C1 condition as compared to any other conditions including A1, A3, A7, C3, and C7 (Additional file 2). As METE is also involved in the synthesis of DNA, RNA, and protein, it seems to help with rapid growth in the early stage under high CO₂ conditions.

There were 18 constitutively downregulated genes including carbonic anhydrase, ferredoxin hydrogenase, and starch synthase (Fig. 2b). The carbonic anhydrase and ferredoxin hydrogenase play essential roles in CCM [13]. Under the conditions of a sufficient external supply of carbon dioxide, the two genes might not need to be upregulated. Additionally, starch synthase was notably downregulated under high CO₂ conditions as carbon storage is not preferred under favorable conditions. Indeed, the carbohydrate content of cells cultivated under ambient conditions was higher (40.7%) compared to those cultivated under 10% CO₂ conditions (32.2%) on day 7 (Additional file 1: Fig. S3).

Gene ontology analysis across different growth phases and CO₂ concentrations

To further understand the function of the DEGs in each phase, Gene Ontology (GO) enrichment analysis was performed. Only the top 7 terms in each category of

biological process (BP), cellular component (CC), and molecular function (MF) are listed (Fig. 3).

The early growth phase on day 1, the photosynthesis and energy-related genes in BP were mainly upregulated under high CO₂ conditions (Fig. 3a). In CC, the genes of chloroplast-related organelles, such as the plastid, chloroplast, and thylakoid, were upregulated. In MF, the chlorophyll binding process is classified as the highly upregulated DEGs. On the other hand, there were no downregulated DEGs under high CO₂ conditions on day 1, except for the glutamine metabolic process (Fig. 3d).

At the mid-exponential phase on day 3, more diverse changes were detected from both upregulated and downregulated DEGs (Fig. 3b and e). In MF, the cells primarily concentrated on protein-level regulation (including catalytic activity, oxidoreductase, chaperone, deacetylase, and phosphatase) under elevated CO₂ conditions. Conversely, transcription-level regulation (such as RNA binding, small molecule binding, and mRNA binding) was downregulated. In addition, both upregulated and downregulated DEGs on day 3 were related to chloroplast and plastid stroma in the CC category. These findings suggest that the cells transitioned to the exponential growth phase on day 3. Indeed, *Chlorella* sp. ABC-001 exhibited accelerated growth under high CO₂ conditions, and this might lead to a halt in the development of photosynthetic function while concentrating on a range of catalytic activities.

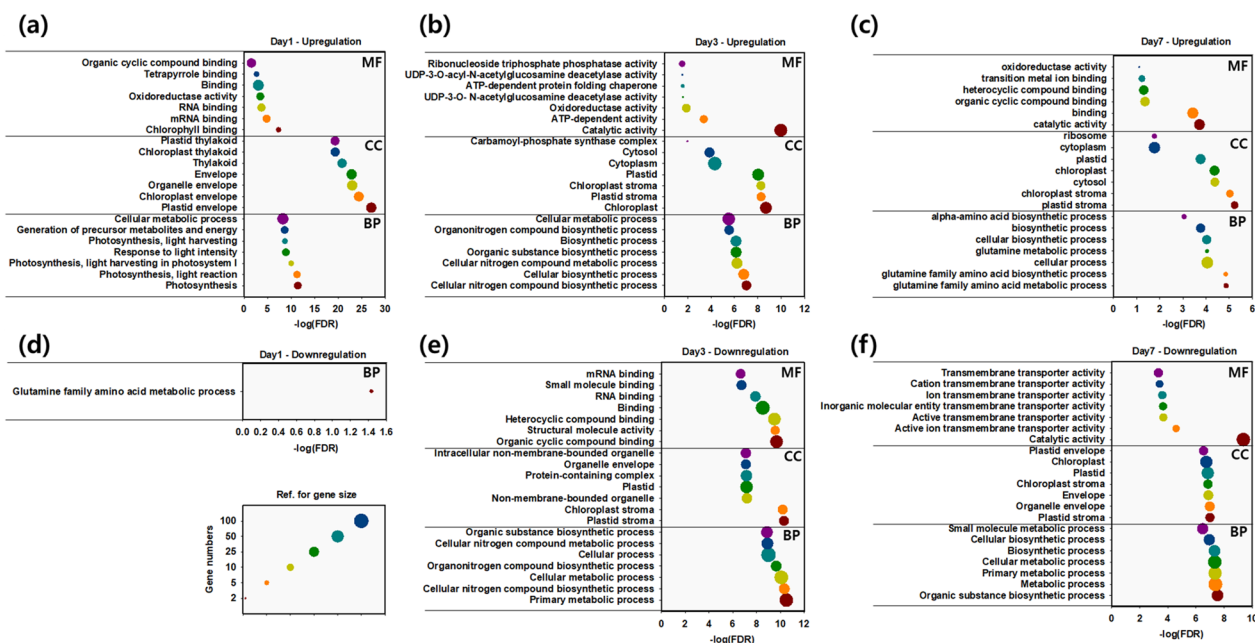


Fig. 3 GO analysis of upregulated and downregulated non-redundant DEGs during cultivation under different CO₂ concentrations. The top 7 terms were listed in each analysis based on the regular growth phase of day 1 (a, d), day 3 (b, e), and day 7 (c, f). The size of the circle represents the gene numbers, and the reference is on the left bottom side of the figure

On day 7, a notable decrease in transmembrane transporter activity was observed in downregulated GO terms for MF under high CO₂ conditions (Fig. 3f). This included diverse transporters such as metal transporters, ATP-binding cassette transporters, sugar transporters, and amino acid transporters (Additional file 2). As photosynthetic activity requires many membrane transporters [42], we expect the decreased photosynthetic activity may heavily cause the decreased membrane transporter activity. The ratio of OD₆₈₀/OD₇₅₀, which serves as an approximate indicator of photosynthetic efficiency and the physiological state of cells with their chlorophyll content [43], displayed a decreasing pattern under high CO₂ conditions after day 3 (Additional file 1: Fig. S4).

In contrast, cells grown under ambient air maintained a consistent OD₆₈₀/OD₇₅₀ ratio, further supporting our explanations.

Transcriptomic profile analysis of CCM and the Calvin cycle

To understand the mechanism behind CO₂ fixation, growth, and lipid production under high CO₂ conditions, we analyzed the associated transcriptomic profiles (Fig. 4). We first looked into the expression patterns of carbonic anhydrase (CA) genes and the Calvin cycle-related genes (Fig. 4). In *Chlorella* sp. ABC-001, 6 CAs were identified, and the CAs generally showed lower expression levels under CO₂-supplemented conditions. Particularly, the CA3 and CA4 showed the most

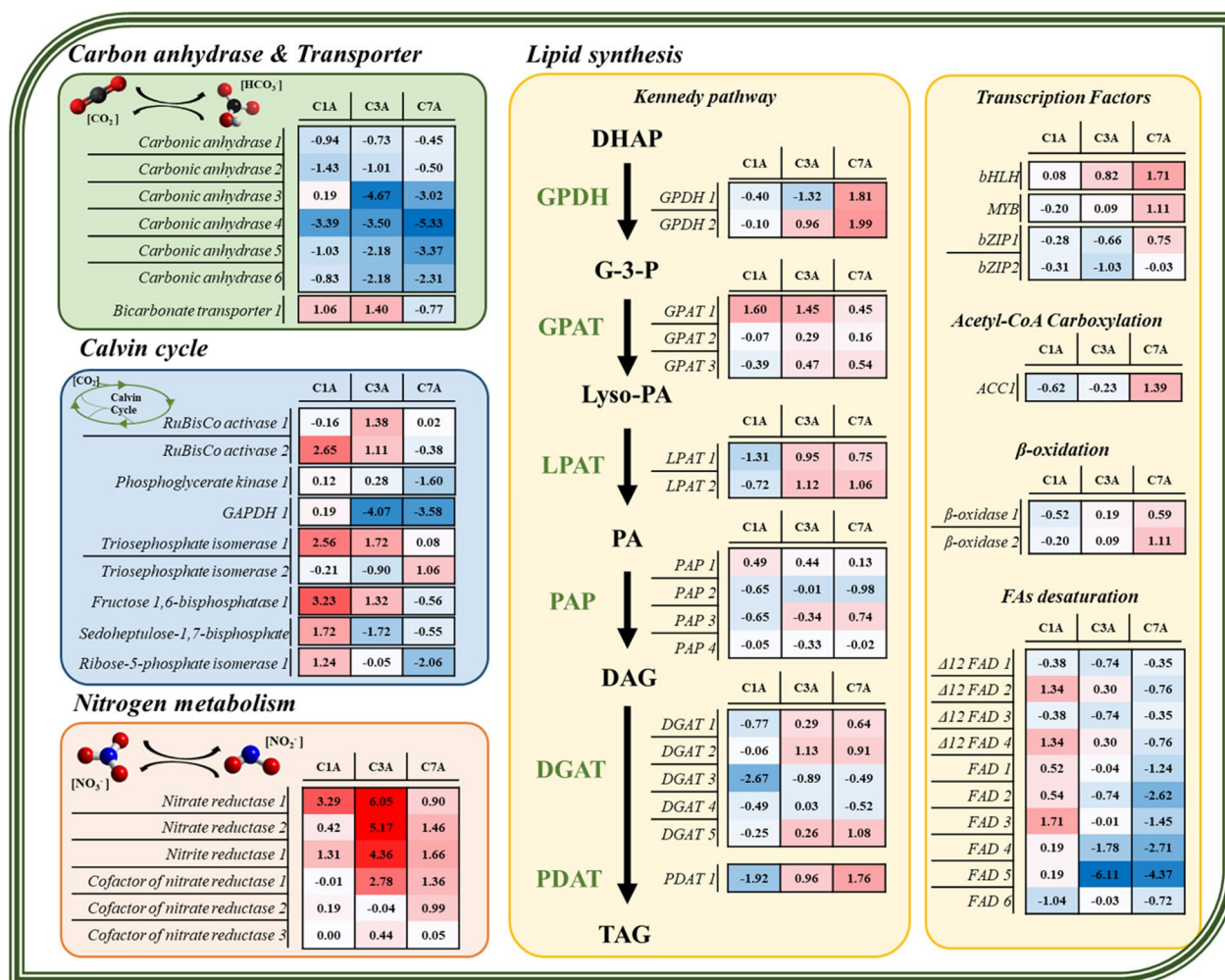


Fig. 4 Relative expression levels (log₂ fold change) of key enzymes participating in carbon fixation, Calvin cycle, nitrogen uptake, and lipid biosynthesis. The Gene IDs of each enzyme are listed in Additional file 1: Table S3. (GAPDH Glyceraldehyde-3-phosphate dehydrogenase, GPDH glycerol-3-phosphate dehydrogenase, GPAT glycerol-3-phosphate acyltransferase, LPAT lysophosphatidic acid acyltransferase, PAP phosphatidic acid phosphohydrolase, DGAT diacylglycerol acyltransferase, PDAT phospholipid-diacylglycerol acyltransferase, bHLH basic helix-loop-helix, MYB myeloblastosis, bZIP basic leucine zipper, ACC1 Acetyl-CoA carboxylase 1, FAD Fatty acid desaturase)

significant changes, 25–40-fold lower expression levels under high CO₂ conditions than under ambient air conditions. This means that the CAs, especially CA3 and CA4, are not necessary under high CO₂ conditions. Conversely, they are expected to play a critical role in the carbon concentrating mechanism under low CO₂ conditions in *Chlorella* sp. ABC-001. The bicarbonate transporter 1, which is an essential transporter for carbon fixation, showed higher expression in high CO₂ conditions on days 1 and 3.

The expression patterns of two potential RuBisCo activases were also analyzed. The RuBisCo activase 1 and 2 showed higher expression levels on day 3 under high CO₂ conditions. In particular, the RuBisCo activase 2 was significantly upregulated on day 1 at the early growth phase. On day 1, most of the genes in the Calvin cycle showed higher expression levels in the CO₂-supplemented culture, whereas it became the opposite on day 7.

Transcriptomic profile analysis of lipid synthesis

In microalgae, nitrogen limitation is the most effective stress to trigger lipid accumulation in the cell [44]. According to Fig. 1c, nitrogen starvation was initiated after day 3 and day 6, under 10% CO₂ and ambient air conditions, respectively. From the RNA-seq comparison of CO₂ vs ambient air, a sudden increase of expression level in nitrate reductase (NR), nitrite reductase (NiR), and cofactor of nitrate reductase (CoNiR) were found on day 3, when nitrogen was almost depleted in 10% CO₂ conditions (Fig. 4). The expression levels of NR, NiR, and CoNiR also consistently increased from day 1 to day 7 in both cultivation conditions (Additional file 1: Fig. S5). High expression levels of NR after nitrogen depletion at the mid-exponential phase have been reported by other researchers as well [13].

Microalgae generally accumulate lipids in the form of tri-acyl-glycerol (TAG), which is synthesized via the Kennedy pathway. Under high CO₂ conditions, FAME contents were almost 40% on day 7, which was 3.1-fold higher than those on day 3 (Fig. 1b). The gene expression patterns of the Kennedy pathway were also related to the phenotypes. The genes encoding for glycerol-3-phosphate dehydrogenase (GPDH), lysophosphatidic acid acyltransferase (LPAT), diacylglycerol acyltransferase (DGAT), and phospholipid-diacylglycerol acyltransferase (PDAT) showed an increased expression level under high CO₂ conditions on day 3 and 7. However, PAP seemed not to be affected much by CO₂ concentrations. A distinct decrease in the expression level of *GPDH*, *LPAT*, *PAP*, *DGAT*, and *PDAT* was observed under 10% CO₂ conditions on day 1. As C1 is the condition that exhibited a very active metabolism in

photosynthesis and energy generation for growth compared to A1 (Figs. 1a and 3a), lipid synthesis seems to be strictly repressed at this point.

In particular, a putative *PDAT* (Csorokiniana-1SL007740t0001) and *GPDH* genes showed the most noticeable changes, which increases the likelihood of its correlation with lipid accumulation. *PDAT*, similar to *DGAT*, delivers an acyl group to diacylglycerol (DAG) in the last step of TAG biosynthesis. However, unlike *DGAT*, which takes acyl-group from acyl-CoA, *PDAT* functions on diverse kinds of substrates such as phospholipids (phosphatidylcholine, phosphatidylethanolamine), membrane lipids (monogalactosyl diacylglycerol, digalactosyl diacylglycerol), and DAG [45]. Accordingly, *GPDH* and *LPAT* are also expected to be important for lipid accumulation according to their increased expression pattern.

We have broadened our analysis to explore additional factors and pathways involved in lipid synthesis in microalgae, not limited to the Kennedy pathway (Fig. 4). Among the transcription factors (TFs) known to promote lipid synthesis in microalgae, basic helix-loop-helix (bHLH) [46] and myeloblastosis (MYB) [47] TFs displayed increased expression profiles under high CO₂ conditions, which correlated with lipid accumulation. In contrast, basic leucine zipper (bZIP) TFs [48] did not exhibit a clear relationship with lipids. Acetyl-CoA carboxylase and β -oxidizing enzymes, responsible for the synthesis and cleavage of acyl-CoA, respectively, showed elevated expression levels under 10% CO₂ conditions during the stationary phase. Additionally, we identified multiple potential fatty acid desaturase (FAD) genes; all 10 FADs consistently demonstrated lower expression levels under high CO₂ conditions on day 7.

Validation of transcriptomic analysis via qRT-PCR

To validate the quality of the RNA-sequencing data obtained in this study, qRT-PCR was carried out by targeting several genes exhibiting different expression patterns (Fig. 5). Indeed, the qRT-PCR results were almost consistent with the RNA-sequencing data. CA3, CA4, and CA5 showed low expression levels under high CO₂ conditions and high expression levels under ambient air conditions by qRT-PCR. Although the expression level of NR1 was lower in qRT-PCR compared to RNA-seq, the overall expression pattern was consistent in both analyses. The CoNiR1 also showed highly conserved expression patterns between qRT-PCR and RNA-sequencing results. Based on these results, we confirmed the credibility of the RNA-sequencing analysis carried out in this study.

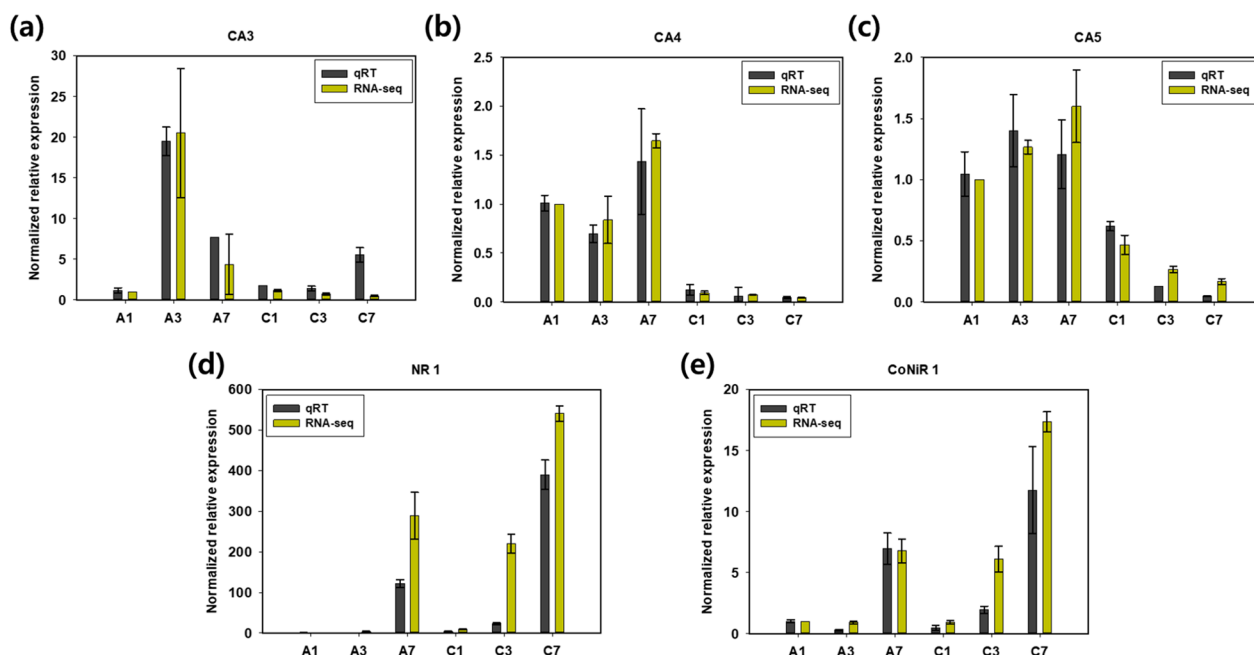


Fig. 5 Validation of RNA-sequencing data by qRT-PCR. Each data was normalized by the expression level of A1. Error bars stand for the standard error calculated from three independent experimental data sets. Specific gene IDs are listed in Additional file 1: Table S3

Discussion

As the potential of *Chlorella* for CO₂ fixation and production of lipids/high value-added substances has been highlighted, a number of transcriptomic approaches have been conducted to elucidate the underlying mechanisms in recent days [13, 17–21, 49, 50]. These researches covered a broad range of areas such as hydrogen photo-production, TAG synthesis, stress tolerance, and starch synthesis. Due to the dynamic activity of cellular metabolism and the formidable amount of transcriptomic data, various interpretations are possible depending on sampling points, comparison groups, and analytic criteria.

In this study, we performed a transcriptomic analysis of *Chlorella* sp. ABC-001 under different CO₂ concentrations (10% CO₂ and ambient air) at three different time points (early exponential, mid-late exponential, and stationary growth phase). From transcriptomic analysis, a total of 10,246 putative genes were annotated, which is an improved result compared to previous studies (9590) on transcriptome profiling of *C. pyrenoidosa* in response to different CO₂ concentrations [20]. Based on the transcriptome data, we illustrated the central carbon metabolism of *Chlorella* sp. ABC-001 with their expression levels at high CO₂ conditions as compared to ambient air conditions according to the time point in Fig. 6.

During the early growth stage under high CO₂ and nutrient conditions, we observed that a high CO₂ level boosted the construction of photosynthetic organelles at

the early stage and upregulated the genes related to the Calvin cycle and bicarbonate transporter to incorporate the inorganic carbon (Figs. 3, 4, and 6). At the same time, nitrate/nitrite reductases were also upregulated as nitrogen is an essential component for chlorophylls under high CO₂ conditions. At the early growth stage (day 1), cells prioritize proliferation while inactivating energy-storage processes, including lipid/starch synthesis and the carbon concentrating mechanism. The intensive expression level of a cobalamin-independent methionine synthase (METE) at the early stage under high CO₂ conditions also supports this idea. METE is the only enzyme that can synthesize methionine in an environment without additional vitamin B₁₂ (cobalamin) [51]. The synthesized methionine is used for protein synthesis and also plays an important role in proliferation by methylation of DNA and RNAs [52, 53]. Fast nitrogen uptake may also be related to methionine synthesis because nitrogen is known to enhance the METE activity by 30–40 folds (Fig. 1c) [54].

From the middle of the exponential phase, cells started downregulating photosynthetic activity under high CO₂ conditions. Particularly, the cells deactivated CCM and decreased the expression level of carbonic anhydrases because they do not need to use tremendous energy for CO₂ transport under high CO₂ conditions. We also found the low expression level of ferredoxin hydrogenase 4 (FeH) located in the chloroplast under high CO₂

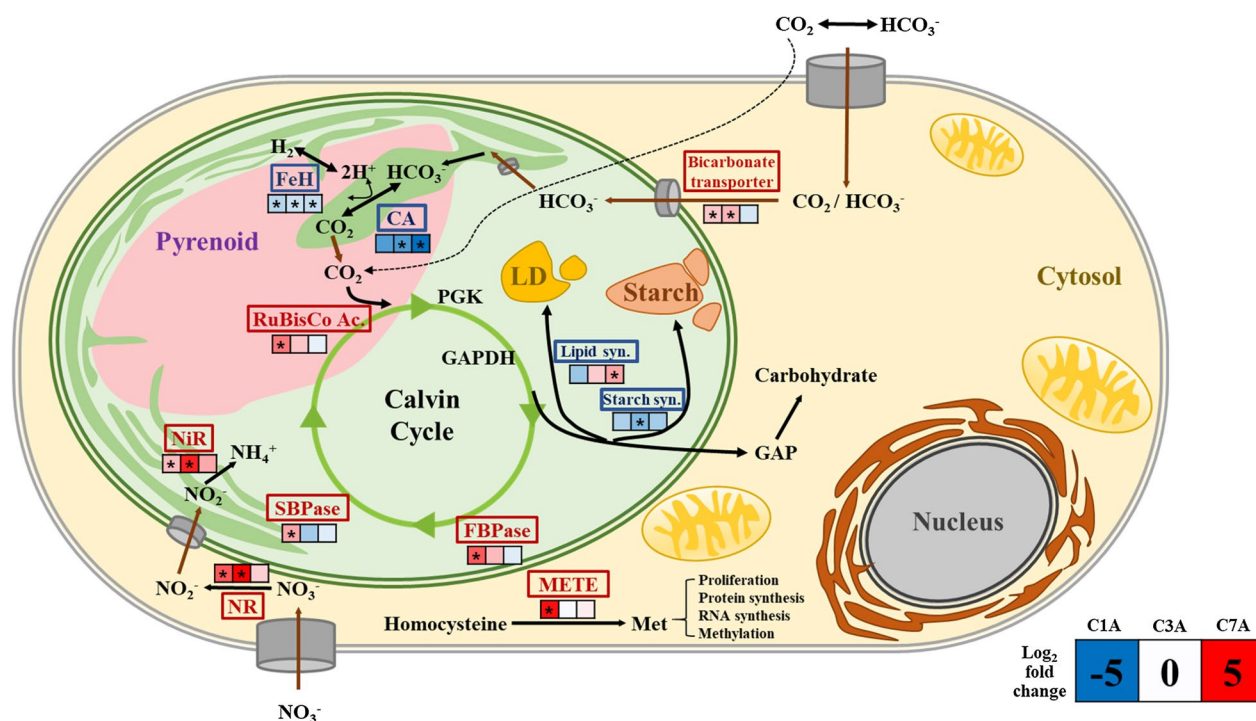


Fig. 6 Overall metabolic changes in *Chlorella* sp. ABC-001 at different CO₂ environments. The color of each enzyme represents either upregulation (red) or downregulation (blue) of genes on day 1. Small boxes stand for the log₂ fold changes of representative enzymes of each metabolic reaction. The asterisk indicates $adj.p < 0.05$. Specific gene IDs are listed in Additional file 1: Table S3. (*FeH* ferredoxin hydrogenase, *SBPase* sedoheptulose-1,7-bisphosphate, *FBPase* fructose 1,6-bisphosphatase, *GAPDH* glyceraldehyde-3-phosphate dehydrogenase, *CA* carbonic anhydrase 4, *NR* nitrate reductase1, *NiR* nitrite reductase1, *METE* cobalamin independent methionine synthase, *Met* methionine, *Lipid syn* represented by PDAT1, *Starch syn* represented by SS)

conditions (Additional file 2). The FeH might catalyze the production of hydrogen ions which is necessary for the reduction of bicarbonate and CO₂ supplement. We also found the upregulation of NR, NiR, and CoNiR according to nitrogen limitation under 10% CO₂ conditions, indicating that the cells subsequently would focus on lipid synthesis.

Chlorella sp. ABC-001 changed gene expression patterns for energy storage in lipids along with nutrient depletion and CO₂ concentrations at the mid-exponential and stationary phases. Indeed, the variations in lipid composition observed in our study cannot be solely attributed to the direct influence of CO₂ concentration. Instead, these results likely represent a complex array of interacting factors. The early onset of nitrogen starvation was primarily instigated by the high CO₂ concentration, contributing to the change in the expression of lipid-related genes. Furthermore, shading effects resulting from high cell concentrations may also play a part in interacting with photosynthetic activity. According to the gene expression patterns under high CO₂ conditions, GPDH and PDAT seemed to play important roles in lipid synthesis. *GPDH1*, *GPDH2*, and *PDAT* were

downregulated at the early growth phase and highly upregulated at the stationary phase, where lipid was significantly accumulated (Fig. 4). Indeed, Yao et al. reported that the overexpression of endogenous GPDH in *Phaeodactylum tricornutum* resulted in a 60% increase in neutral lipids [55]. *PDAT* usually exists as a single-copy gene, even in oleaginous strains [56] and it has been suggested that *PDAT* contributes to TAG synthesis in *Chlamydomonas reinhardtii*, *Myrmecia incisa* and *Nannochloropsis* [45, 57, 58]. Recently, engineering of *PDAT* was actually proven to be effective for increasing the TAG contents in *Nannochloropsis* [58, 59]. The fatty acid composition of lipids also supported the transcriptomic and phenotypic data (Additional file 1: Fig. S6). On day 7, α -linolenic acid (C18:3) decreased, while oleic acid (C18:1) increased under 10% CO₂ conditions. The change in fatty acid composition might be primarily attributed to the consistently lower expression levels of multiple FADs (Fig. 4). Additionally, the degradation of chloroplasts may contribute to the fatty acid composition, as polyunsaturated fatty acids are the primary components of membrane lipids [60, 61]. Consequently, fatty acids and acyl-groups from degraded membrane lipids, which

correspond well with increased β -oxidase expression, can be used for de novo TAG synthesis by PDAT. Thus, the putative PDAT gene (Csorokiniana1SL007740t0001) showing a high expression level at the lipid accumulation stage in *Chlorella* sp. ABC-001 can be a promising genetic target for lipid production in microalgae.

Generally, DGAT genes have been studied well in microalgae because DGAT is in charge of the last step for lipid synthesis, transferring the acyl group to DAG for TAG synthesis. DGAT genes often exist with multiple copies in microalgae, and only some of them were proven to be effective in enhancing lipid accumulation [62, 63]. We also identified 5 DGAT genes in *Chlorella* sp. ABC-001. However, their expression patterns were not consistent with the lipid accumulation phenotype. Although the expression patterns of DGAT1, DGAT2, and DGAT5 are similar to the lipid accumulation pattern, the expression levels were not as high as that of GPDH and PDAT. This pattern was similar to GPAT and LPAT. Thus, The DGAT, GPAT, and LPAT from *Chlorella* sp. ABC-001 might not be suitable target genes for lipid synthesis.

Taken together, our analysis successfully elucidated the relationship between the phenotypic and transcriptomic changes of *Chlorella* sp. ABC-001 in response to CO₂ conditions across various growth phases. Moreover, we identified key genes involved in carbon concentration mechanism (CCM), cell development, and lipid accumulation under high CO₂ conditions. This study provides high-quality transcriptomic data that can be applied in microalgal synthetic biology and metabolic engineering for industrial purposes, particularly in utilizing industrial exhaust gas containing high CO₂ concentrations. Our time-course transcriptomic analysis (days 1, 3, and 7) addresses a gap in the current research landscape, shedding light on the molecular mechanisms underlying long-term adaptations. While many studies focus on shorter time frames (24 or 48 h), we deliver a more comprehensive understanding of metabolic changes and adaptations over extended periods, better representing industrial microalgal cultivation conditions.

Conclusions

To address climate change issues, it is crucial to research the production of high-value materials utilizing industrial flue gases. However, conventional microalgae typically do not have high CO₂ tolerance. In this study, we analyzed the transcriptome of *Chlorella* ABC-001, a high CO₂ tolerant strain, over an extended period (7 days) during which considerable lipid accumulation occurred under high CO₂ conditions. We confirmed that *Chlorella* sp. ABC-001 focuses on fast growth at the early stage under high CO₂ conditions by upregulating the Calvin cycle, METE, and bicarbonate transporters. However,

CA expression was decreased because CCM did not need to be significantly activated in the high CO₂ supply. In addition, our transcriptomic analysis revealed that PDAT and GPDH, the first and final genes for TAG synthesis, are expected to play a crucial role in lipid synthesis under high CO₂ conditions. This in-depth knowledge can contribute to developing more efficient microalgal cultivation strategies and innovative genetic engineering approaches for enhancing growth and lipid production capabilities.

Materials and methods

Strains and cultivation

Chlorella sp. ABC-001, a marine microalgae isolated from a coastal region in Jeju island (South Korea) was used in this study [39]. This species was chosen for its high CO₂ tolerance, and the transcriptomic differences were analyzed under both aerobic and 10% CO₂-supplied conditions [38]. The cells were maintained and cultivated in N8 media (1 g L⁻¹ KNO₃, 0.74 g L⁻¹ Na₂HPO₄·2H₂O, 13 mg L⁻¹ CaCl₂·2H₂O, 10 mg L⁻¹ FeEDTA, 50 mg L⁻¹ MgSO₄·7H₂O, 12.98 mg L⁻¹ MnCl₂·4H₂O, 3.2 mg L⁻¹ ZnSO₄·7H₂O, 1.83 mg L⁻¹ CuSO₄·5H₂O, 3.58 mg L⁻¹ Al₂(SO₄)₃·18H₂O) through the whole experiments. The cultivation was performed in 500 mL column PBRs (photobioreactors) with working volumes of 400 mL under 200 μ mol photons m⁻² s⁻¹ of light at 30 °C. The initial concentrations in each experiment were fixed at 5 × 10⁶ cells mL⁻¹. For aerobic conditions, ambient air was supplied at 0.6 vvm (volume gas per volume medium per minute), whereas 0.6 vvm of 10% CO₂ was supplied for CO₂-sufficient conditions.

Cultivational analysis

The growth of cells was measured daily in terms of cell density and dried cell weight (DCW) using a Cellometer (Auto X4, Nexcelom, USA) and filter paper (Whatman, USA) as described in previous publications [64]. The optical densities at wavelengths of 680 nm and 750 nm were measured using a UV-VIS spectrophotometer (UV-1800, Shimadzu, Japan). Accumulated lipids were determined by gas-chromatography (HP 6890; Agilent Technologies, CA, USA) after extraction and transesterification through the Bligh-Dyer method similar to our previous research [65]. The remaining nutrients in the media, particularly nitrate and sulfate, were measured with an elemental analyzer (FLASH 2000 series; Thermo Scientific, MA, USA) at the KAIST Analysis Center for Research Advancement [66]. The total carbohydrate content was quantified using the phenol-sulfuric acid method described in a previous study [38]. In brief, approximately 3–5 mg of dried biomass powder was weighed, thoroughly mixed in 10 mL of distilled

water, and then 1 mL of the mixture was transferred to clean glass tubes. Next, 1 mL of 5% wt. phenol solution and 5 mL of concentrated sulfuric acid were added, and the tubes were left in the dark for 30 min to facilitate the reaction. The tubes were inverted several times to mix the solution well, and the absorbance at 470 nm was measured using a UV/Vis spectrophotometer (Shimadzu, Japan).

Transcriptomic analysis

RNA extraction, RNA sequencing, and annotations

The cultivated cells were harvested on days 1, 3, and 7 in each condition and were homogenized with a bead beater (Percellys 24, Bertin Technologies, Paris, France). Using NucleoZOL (Macherey–Nagel, Düren, Germany) according to the provided protocol, RNA was extracted from the homogenized cells. gDNA was then removed from the collected RNAs using DNA-free™ DNase kits (Ambion, TX, USA). Finally, cDNA was synthesized using an oligo (dT) 20 primer (Invitrogen, CA, USA) and Superscript III™ Reverse Transcriptase (Invitrogen, CA, USA).

RNA-seq was conducted using an Illumina HiSeq2500, and 18 FASTQ files of sequences were yielded (A1, A3, A7, C1, C3, C7, three biological replicates per condition). Then, the transcriptome short reads were pre-treated using DynamicTrim and LengthSort provided by the Solera QA package to sort out low-quality reads. The resulting clean-reads were assembled by Velvet (ver. 1.2.08) and Oases (ver.0.2.08) according to the provided protocols [67, 68]. The quality of RNA was assured by statistics of dynamic trim (Additional file 3), length sort (Additional file 3), final assembled transcripts (Additional file 3), and RNA integrity electropherograms (Additional file 1: Fig. S7). Annotation was conducted using BLASTX against amino acids from a diverse database including Phytozome v9, NCBI NR, Uniprotkb, KOG, and KEGG ($e \leq 1e^{-10}$). InterProScan was carried out using tools provided by EMBL as the default option.

Analysis of DEGs

For the selected clean reads, the read counts were calculated through mapping using Bowtie2 (v2.1.0) software (mismatch < 2 bp, penalty) [69]. Samples with high deviations were normalized by DEseq using R (Additional file 1: Fig. S8) [70]. Differentially expressed genes (DEGs) of *Chlorella* sp. ABC-001 during cultivation were selected according to the twofold change method and binomial method, where the criteria were set as ‘adjusted *P*-value (FDR) < 0.01’. When the \log_2 value of the fold change was higher than 1, it was annotated as an ‘up-regulation’, and when the value was lower than -1, it was annotated as a ‘down-regulation’. For GO (gene ontology) analysis, the

selected DEGs were aligned to the sequences from the GO database and processed through Blast2GO. The significance level was set at 0.05 and categorized into three functional categories of BP (biological process), CC (Cellular component), and MF (molecular function). DEGs were annotated by BLASTX ($e \leq 1e^{-10}$, Best hits) against amino acid sequences from KEGG DB. The selected DEGs are described by the MA plot in Additional file 1: Fig. S9.

Quantitative real-time PCR (qRT-PCR) validation

The cDNA prepared for RNA sequencing was also used as a qRT-PCR template for validation. The housekeeping gene for TATA-box binding protein (*TATA*) was used as a control. All the primers used for qRT-PCR are listed in Additional file 1: Table S2. qRT-PCR was performed with 20 μ L reaction volumes containing 2 μ L of cDNAs (20 ng), 0.5 μ L of each primer (10 μ M), and 10 μ L of Universal SYBR supermix (Bio-Rad, USA). The mixture was loaded on 96-well Hard Shell PCR plates (Bio-Rad, USA) and analyzed using a CFX96 Real-Time system (Bio-Rad, USA).

Statistic analysis

Three biological replicates were performed for all experiments, with results presented as mean \pm standard error (SE). Statistical analysis was performed using an in-house script for DEG selection and metaboanalyst 5.0 (*t*-test, FDR) for other experimental data [71]. Detailed explanations for each case are described in the “Analysis of DEGs” section and legends of each figure.

Abbreviations

GO	Gene ontology
BP	Biological process
CC	Cellular component
MF	Molecular function
DEG	Differentially expressed genes
CCM	Carbon concentrating mechanism
FDR	False discovery rate
CA	Carbonic anhydrase
GPDH	Glycerol-3-phosphate dehydrogenase
GPAT	Glycerol-3-phosphate acyltransferase
LPAT	Lysophosphatidic acid acyltransferase
PAP	Phosphatidic acid phosphohydrolase
DGAT	Diacylglycerol acyltransferase
PDAT	Phospholipid-diacylglycerol acyltransferase
GAPDH	Glyceraldehyde-3-phosphate dehydrogenase
RuBisCo	Ribulose-1,5-bisphosphate carboxylase
TAG	Triacylglycerol
DAG	Diacylglycerol
METE	Cobalamine-independent methionine synthase
bHLH	Basic helix-loop-helix
MYB	Myeloblastosis
bZIP	Basic leucine zipper
ACC1	Acetyl-CoA carboxylase 1
FAD	Fatty acid desaturase

Supplementary Information

The online version contains supplementary material available at <https://doi.org/10.1186/s13068-023-02358-4>.

Additional file 1: Fig. S1–S9, Tables S1–S3. Fig. S1 Pairs plot analysis for examining the reproducibility of data sets. **a** A1D, **b** A3D, **c** A7D, **d** C1D, **e** C3D, **f** C7D. **Fig. S2** Gene ratio by species of genes used to annotate representative transcripts using NCBI NR. **Fig. S3** Carbohydrate content of cells cultivated under ambient air conditions and 10% CO₂ conditions on day 7. **Fig. S4** The changes in OD680/OD750 during the whole cultivation period. The ratio of OD680/OD750 is an approximate indicator of the photosynthetic efficiency and the physiological state of the cells in terms of their chlorophyll contents. **Fig. S5** Relative expression levels (log₂ fold change) of key enzymes participating in carbon fixation, Calvin cycle, nitrogen uptake, and lipid biosynthesis. Time-course comparison of cells cultivated in the same CO₂ concentration (10% CO₂ or ambient air) at different growth phase. **Fig. S6** The profiles of fatty acid composition of cells under A3D, A7D, C3D, and C7D conditions. Error bars stand for the standard error calculated from three independent experimental data sets. **Fig. S7** The RNA integrity electropherograms of each sample. **Fig. S8** Boxplot of gene expression level before and after normalization. **a** Average expression level of the raw data from each sample **b** Average expression level of the normalized data from each sample. **Fig. S9** MA plot of DEGs in each condition. X-axis represents the average expression value of the control and sample on a log₂ scale, and the Y-axis represents the fold change between the two samples, on a log₂ scale. **Table S1** Statistical results of annotated final unigenes. **Table S2** Primers used in this study for qRT-PCR. **Table S3** Gene IDs of key enzymes described in Figs. 4, 5 and 6.

Additional file 2: Transcription levels of unigenes and DEGs.

Additional file 3: Detailed information of transcriptome sequencing data.

Acknowledgements

Not applicable.

Author contributions

HGK, BL and NKK designed the whole experimental scheme. HGK cultivated the microalgae and collected relevant data. SJ extracted the RNA from the harvested cells. JMC analyzed the carbohydrate contents of cells. HGK analyzed the transcriptomic data and wrote the original draft manuscript. HGK, JMC, SJ, YC, BL and NKK revised the manuscript. All authors read and approved the final manuscript.

Funding

This work was supported by the Commercialization Promotion Agency for R&D Outcomes (COMPA) grant funded by the Korea government (MSIT) (2023B200 and 2023B220), the National Research Foundation of Korea (NRF) Grant funded by the Ministry of Science and ICT, Korea government (2021 R1F1A10512751331482093800103), the C1 Gas Refinery Program through the National Research Foundation of Korea (NRF) funded by the Ministry of Science and ICT (2015M3D3A1A01064882), Basic Science Research Capacity Enhancement Project through Korea Basic Science Institute (National Research Facilities and Equipment Center) grant funded by the Ministry of Education (No. 2019R1A6C101052), and a grant from Kyung Hee University in 2022 (KHU-20222217).

Availability of data and materials

The datasets generated during the current study are available at NCBI under BioProject accession code PRJNA757763.

Declarations

Ethics approval and consent to participate

Not applicable.

Consent for publication

Not applicable.

Competing interests

The authors declare that they have no competing interests.

Author details

¹Carl R. Woese Institute for Genomic Biology, University of Illinois at Urbana-Champaign, Urbana, IL, USA. ²Department of Chemical and Biomolecular Engineering, KAIST, 291 Daehak-ro, Yuseong-gu, Daejeon 34141, Republic of Korea. ³Department of Microbial Biotechnology, College of Science and Technology, Mokwon University, 88 Doanbuk-ro, Seo-gu, Daejeon 35349, Republic of Korea. ⁴Department of Chemical Engineering, College of Engineering, Kyung Hee University, Yongin 17104, Republic of Korea.

Received: 21 March 2023 Accepted: 11 June 2023

Published online: 15 July 2023

References

- Singh UB, Ahluwalia AS. Microalgae: a promising tool for carbon sequestration. *Mitig Adapt Strat Glob Change*. 2013;18(1):73–95.
- Packer M. Algal capture of carbon dioxide; biomass generation as a tool for greenhouse gas mitigation with reference to New Zealand energy strategy and policy. *Energy Policy*. 2009;37(9):3428–37.
- International Energy Agency. State of Technology Review on Algae Bioenergy. 2017. <https://www.ieabioenergy.com/wp-content/uploads/2017/01/EA-Bioenergy-Algae-report-update-20170114.pdf>
- Morales M, Sánchez L, Revah S. The impact of environmental factors on carbon dioxide fixation by microalgae. *FEMS Microbiol Lett*. 2018;365(3).
- Gerotto C, Norici A, Giordano M. Toward enhanced fixation of CO₂ in aquatic biomass: focus on microalgae. *Front Energy Res*. 2020. <https://doi.org/10.3389/fenrg.2020.00213>.
- Zhu B, Chen G, Cao X, Wei D. Molecular characterization of CO₂ sequestration and assimilation in microalgae and its biotechnological applications. *Biores Technol*. 2017;244:1207–15.
- Choi HI, Hwang SW, Kim J, Park B, Jin E, Choi IG, Sim SJ. Augmented CO₂ tolerance by expressing a single H(+)-pump enables microalgal valorization of industrial flue gas. *Nat Commun*. 2021;12(1):6049.
- Mistry AN, Ganta U, Chakrabarty J, Dutta S. A review on biological systems for CO₂ sequestration: organisms and their pathways. *Environ Prog Sustain Energy*. 2019;38(1):127–36.
- Mortensen LM, Gislerød HR. The growth of *Chlamydomonas reinhardtii* as influenced by high CO₂ and low O₂ in flue gas from a silicomanganese smelter. *J Appl Phycol*. 2015;27(2):633–8.
- Song C, Pan W, Srimat ST, Zheng J, Li Y, Wang Y-H, Xu B-Q, Zhu Q-M. Tri-reforming of methane over Ni catalysts for CO₂ conversion to syngas with desired H₂/CO ratios using flue gas of power plants without CO₂ separation. *Stud Surf Sci Catal*. 2004;153:315–22.
- Kadam KL. Environmental implications of power generation via coal-microalgae cofiring. *Energy*. 2002;27(10):905–22.
- Guccione A, Biondi N, Sampietro G, Rodolfi L, Bassi N, Tedrini MR. *Chlorella* for protein and biofuels: from strain selection to outdoor cultivation in a Green Wall Panel photobioreactor. *Biotechnol Biofuels*. 2014;7:84–84.
- Huang Y, Cheng J, Lu HX, He Y, Zhou JH, Cen KF. Transcriptome and key genes expression related to carbon fixation pathways in *Chlorella* PY-ZU1 cells and their growth under high concentrations of CO₂. *Biotechnol Biofuels*. 2017;10:1.
- Kim J, Chang KS, Lee S, Jin E. Establishment of a genome editing tool using CRISPR-Cas9 in *Chlorella vulgaris* UTEX395. *Int J Mol Sci*. 2021;22(2):480.
- Ji L, Fan J. Electroporation procedures for genetic modification of green algae (*Chlorella* spp.). In: Li S, Chang L, Teissie J, editors. *Electroporation protocols: microorganism, mammalian system, and nanodevice*. New York: Springer US; 2020. p. 181–5.
- Cha TS, Yee W, Aziz A. Assessment of factors affecting agrobacterium-mediated genetic transformation of the unicellular green alga, *Chlorella vulgaris*. *World J Microbiol Biotechnol*. 2012;28(4):1771–9.
- Li L, Zhang GQ, Wang QH. De novo transcriptomic analysis of *Chlorella sorokiniana* reveals differential genes expression in photosynthetic carbon fixation and lipid production. *BMC Microbiol*. 2016;16:1.

18. Nordin N, Yusof N, Maeda T, Mustapha NA, Mohd Yusoff MZ, Raja Khairuddin RF. Mechanism of carbon partitioning towards starch and triacylglycerol in *Chlorella vulgaris* under nitrogen stress through whole-transcriptome analysis. *Biomass Bioenerg*. 2020;138:105600.
19. Huang W, Ye J, Zhang J, Lin Y, He M, Huang J. Transcriptome analysis of *Chlorella zofingiensis* to identify genes and their expressions involved in astaxanthin and triacylglycerol biosynthesis. *Algal Res*. 2016;17:236–43.
20. Sun X, Shen J, Bai FW, Xu NJ. Transcriptome profiling of the microalga *Chlorella pyrenoidosa* in response to different carbon dioxide concentrations. *Mar Genom*. 2016;29:81–7.
21. Fan J, Xu H, Li Y. Transcriptome-based global analysis of gene expression in response to carbon dioxide deprivation in the green algae *Chlorella pyrenoidosa*. *Algal Res*. 2016;16:12–9.
22. Mansfeldt CB, Richter LV, Ahner BA, Cochlan WP, Richardson RE. Use of de novo transcriptome libraries to characterize a novel oleaginous marine chlorella species during the accumulation of triacylglycerols. *PLoS ONE*. 2016;11(2):e0147527.
23. Wang R, Miao X. Lipid turnover and SQUAMOSA promoter-binding proteins mediate variation in fatty acid desaturation under early nitrogen deprivation revealed by lipidomic and transcriptomic analyses in *Chlorella pyrenoidosa*. *Front Plant Sci*. 2022;13:987354.
24. Zhu Q, Zhang M, Liu B, Wen F, Yang Z, Liu J. Transcriptome and metabolome profiling of a novel isolate *Chlorella sorokiniana* G32 (Chlorophyta) displaying enhanced starch accumulation at high growth rate under mixotrophic condition. *Front Microbiol*. 2021;12:760307.
25. Li H, Tan J, Mu Y, Gao J. Lipid accumulation of *Chlorella* sp. TLD6B from the taklimakan desert under salt stress. *PeerJ*. 2021;9:e11525.
26. Poong S-W, Lee K-K, Lim P-E, Pai T-W, Wong C-Y, Phang S-M, Chen C-M, Yang C-H, Liu C-C. RNA-Seq-mediated transcriptomic analysis of heat stress response in a polar *Chlorella* sp. (Trebouxiophyceae, Chlorophyta). *J Appl Phycol*. 2018;30:3103–19.
27. Zhang Y, Chen Z, Tao Y, Wu W, Zeng Y, Liao K, Li X, Chen L. Transcriptomic and physiological responses of *Chlorella pyrenoidosa* during exposure to 17 α -ethynylestradiol. *Int J Mol Sci*. 2022;23(7):3583.
28. Cheng D, Li X, Yuan Y, Yang C, Tang T, Zhao Q, Sun Y. Adaptive evolution and carbon dioxide fixation of *Chlorella* sp. in simulated flue gas. *Sci Total Environ*. 2019;650(Pt 2):2931–8.
29. Hu X, Zhou J, Liu G, Gui B. Selection of microalgae for high CO₂ fixation efficiency and lipid accumulation from ten *Chlorella* strains using municipal wastewater. *J Environ Sci*. 2016;46:83–91.
30. Cheng J, Huang Y, Feng J, Sun J, Zhou J, Cen K. Mutate *Chlorella* sp. by nuclear irradiation to fix high concentrations of CO₂. *Bioresour Technol*. 2013;136:496–501.
31. Raven JA, Giordano M, Beardall J, Maberly SC. Algal evolution in relation to atmospheric CO₂: carboxylases, carbon-concentrating mechanisms and carbon oxidation cycles. *Philos Trans R Soc Lond B Biol Sci*. 2012;367(1588):493–507.
32. Kang NK, Baek K, Koh HG, Atkinson CA, Ort DR, Jin Y-S. Microalgal metabolic engineering strategies for the production of fuels and chemicals. *Biores Technol*. 2022;345:126529.
33. Xu Y. Biochemistry and biotechnology of lipid accumulation in the microalga *Nannochloropsis oceanica*. *J Agric Food Chem*. 2022;70(37):11500–9.
34. Zulu NN, Zienkiewicz K, Vollheyde K, Feussner I. Current trends to comprehend lipid metabolism in diatoms. *Prog Lipid Res*. 2018;70:1–16.
35. Azaman SNA, Wong DCJ, Tan SW, Yusoff FM, Nagao N, Yeap SK. De novo transcriptome analysis of *Chlorella sorokiniana*: effect of glucose assimilation, and moderate light intensity. *Sci Rep*. 2020;10(1):17331.
36. Qu D, Miao X. Carbon flow conversion induces alkali resistance and lipid accumulation under alkaline conditions based on transcriptome analysis in *Chlorella* sp. *BLD. Chemosphere*. 2021;265: 129046.
37. Abdellaoui N, Kim MJ, Choi TJ. Transcriptome analysis of gene expression in *Chlorella vulgaris* under salt stress. *World J Microbiol Biotechnol*. 2019;35(9):141.
38. Cho JM, Oh YK, Park WK, Chang YK. Effects of nitrogen supplementation status on CO₂ biofixation and biofuel production of the promising microalga *Chlorella* sp. ABC-001. *J Microbiol Biotechnol*. 2020;30(8):1235–43.
39. Yong Keun Chang JMC, Lee B, Kim EK, Moon M. *Chlorella* sp. ABC-001 strain having excellent lipid productivity and cell growth rate under high carbon dioxide and salt concentration condition and uses thereof. In: South Korea. <https://patents.google.com/patent/KR101855733B1/en>
40. Solovchenko A, Khozin-Goldberg I. High-CO₂ tolerance in microalgae: possible mechanisms and implications for biotechnology and bioremediation. *Biotechnol Lett*. 2013;35(11):1745–52.
41. Holden HM, Thoden JB, Rauschel FM. Carbamoyl phosphate synthetase: an amazing biochemical odyssey from substrate to product. *Cell Mol Life Sci CMLS*. 1999;56(5):507–22.
42. Babla M, Cai S, Chen G, Tissue DT, Cazzonelli CI, Chen ZH. Molecular evolution and interaction of membrane transport and photoreception in plants. *Front Genet*. 2019;10:956.
43. Sivakaminathan S, Hankamer B, Wolf J, Yarnold J. High-throughput optimisation of light-driven microalgae biotechnologies. *Sci Rep*. 2018;8(1):11687.
44. Wang X, Fosse HK, Li K, Chauton MS, Vadstein O, Reitan KI. Influence of nitrogen limitation on lipid accumulation and EPA and DHA content in four marine microalgae for possible use in aquafeed. *Front Marine Sci*. 2019. <https://doi.org/10.3389/fmars.2019.00095>.
45. Yoon K, Han D, Li Y, Sommerfeld M, Hu Q. Phospholipid:diacylglycerol acyltransferase is a multifunctional enzyme involved in membrane lipid turnover and degradation while synthesizing triacylglycerol in the unicellular green microalga *Chlamydomonas reinhardtii*. *Plant Cell*. 2012;24(9):3708–24.
46. Kang NK, Jeon S, Kwon S, Koh HG, Shin SE, Lee B, Choi GG, Yang JW, Jeong BR, Chang YK. Effects of overexpression of a bHLH transcription factor on biomass and lipid production in *Nannochloropsis salina*. *Biotechnol Biofuels*. 2015;8:200.
47. Shi M, Yu L, Shi J, Liu J. A conserved MYB transcription factor is involved in regulating lipid metabolic pathways for oil biosynthesis in green algae. *New Phytol*. 2022;235(2):576–94.
48. Kwon S, Kang NK, Koh HG, Shin SE, Lee B, Jeong BR, Chang YK. Enhancement of biomass and lipid productivity by overexpression of a bZIP transcription factor in *Nannochloropsis salina*. *Biotechnol Bioeng*. 2018;115(2):331–40.
49. Zhou L, Cheng D, Wang L, Gao J, Zhao Q, Wei W, Sun Y. Comparative transcriptomic analysis reveals phenol tolerance mechanism of evolved *Chlorella* strain. *Biores Technol*. 2017;227:266–72.
50. Li L, Zhang L, Gong F, Liu J. Transcriptomic analysis of hydrogen photo-production in *Chlorella pyrenoidosa* under nitrogen deprivation. *Algal Res*. 2020;47:101827.
51. Ellis KA, Cohen NR, Moreno C, Marchetti A. Cobalamin-independent methionine synthase distribution and influence on vitamin B12 growth requirements in marine diatoms. *Protist*. 2017;168(1):32–47.
52. Nef C, Jung S, Mairat F, Kaas R, Grizeau D, Garnier M. How haptophytes microalgae mitigate vitamin B-12 limitation. *Sci Rep*. 2019;9:8417.
53. Kumar S, Mohapatra T. Dynamics of DNA methylation and its functions in plant growth and development. *Front Plant Sci*. 2021;12:596236.
54. Bertrand EM, Moran DM, McIlvin MR, Hoffman JM, Allen AE, Saito MA. Methionine synthase interreplacement in diatom cultures and communities: implications for the persistence of B-12 use by eukaryotic phytoplankton. *Limnol Oceanogr*. 2013;58(4):1431–50.
55. Yao Y, Lu Y, Peng KT, Huang T, Niu YF, Xie WH, Yang WD, Liu JS, Li HY. Glycerol and neutral lipid production in the oleaginous marine diatom *Phaeodactylum tricorutum* promoted by overexpression of glycerol-3-phosphate dehydrogenase. *Biotechnol Biofuels*. 2014;7:1.
56. Wang D, Ning K, Li J, Hu J, Han D, Wang H, Zeng X, Jing X, Zhou Q, Su X, et al. *Nannochloropsis* genomes reveal evolution of microalgal oleaginous traits. *PLoS Genet*. 2014;10(1):e1004094.
57. Liu XY, Ouyang LL, Zhou ZG. Phospholipid: diacylglycerol acyltransferase contributes to the conversion of membrane lipids into triacylglycerol in *Myrmecia incisa* during the nitrogen starvation stress. *Sci Rep-Uk*. 2016;6:1.
58. Yang J, Liu J, Pan Y, Maréchal E, Amato A, Liu M, Gong Y, Li Y, Hu H. PDAT regulates PE as transient carbon sink alternative to triacylglycerol in *Nannochloropsis*. *Plant Physiol*. 2022;189(3):1345–62.
59. Fattore N, Bucci F, Bellan A, Bossi S, Maffei ME, Morosinotto T. An increase in the membrane lipids recycling by PDAT overexpression stimulates the accumulation of triacylglycerol in *Nannochloropsis gaditana*. *J Biotechnol*. 2022;357:28–37.
60. Sukenik A, Carmeli Y, Berner T. Regulation of fatty acid composition by irradiance level in the eustigmatophyte *Nannochloropsis* sp.1. *J Phycol*. 1989;25(4):686–92.

61. Ma X-N, Chen T-P, Yang B, Liu J, Chen F. Lipid production from *Nannochloropsis*. *Mar Drugs*. 2016;14(4):61.
62. Hung C-H, Ho M-Y, Kanehara K, Nakamura Y. Functional study of diacylglycerol acyltransferase type 2 family in *Chlamydomonas reinhardtii*. *Febs Lett*. 2013;587(15):2364–70.
63. Cui Y, Zhao J, Wang Y, Qin S, Lu Y. Characterization and engineering of a dual-function diacylglycerol acyltransferase in the oleaginous marine diatom *Phaeodactylum tricornutum*. *Biotechnol Biofuels*. 2018;11(1):32.
64. Koh HG, Kang NK, Jeon S, Shin SE, Jeong BR, Chang YK. Heterologous synthesis of chlorophyll b in *Nannochloropsis salina* enhances growth and lipid production by increasing photosynthetic efficiency. *Biotechnol Biofuels*. 2019;12:122.
65. Jeon S, Koh HG, Cho JM, Kang NK, Chang YK. Enhancement of lipid production in *Nannochloropsis salina* by overexpression of endogenous NADP-dependent malic enzyme. *Algal Res*. 2021;54:102218.
66. Kwak M, Roh S, Yang A, Lee H, Chang YK. High shear-assisted solvent extraction of lipid from wet biomass of *Aurantiochytrium* sp. KRS101. *Sep Purif Technol*. 2019;227:115666.
67. Zerbino DR, Birney E. Velvet: algorithms for de novo short read assembly using de Bruijn graphs. *Genome Res*. 2008;18(5):821–9.
68. Schulz MH, Zerbino DR, Vingron M, Birney E. Oases: robust de novo RNA-seq assembly across the dynamic range of expression levels. *Bioinformatics*. 2012;28(8):1086–92.
69. Langmead B, Salzberg SL. Fast gapped-read alignment with Bowtie 2. *Nat Methods*. 2012;9(4):357–9.
70. Anders S, Huber W. Differential expression analysis for sequence count data. *Genome Biol*. 2010;11(10):R106.
71. Pang Z, Chong J, Zhou G, de Lima Morais DA, Chang L, Barrette M, Gauthier C, Jacques P-É, Li S, Xia J. MetaboAnalyst 5.0: narrowing the gap between raw spectra and functional insights. *Nucleic Acids Res*. 2021;49(W1):W388–96.

Publisher's Note

Springer Nature remains neutral with regard to jurisdictional claims in published maps and institutional affiliations.

Ready to submit your research? Choose BMC and benefit from:

- fast, convenient online submission
- thorough peer review by experienced researchers in your field
- rapid publication on acceptance
- support for research data, including large and complex data types
- gold Open Access which fosters wider collaboration and increased citations
- maximum visibility for your research: over 100M website views per year

At BMC, research is always in progress.

Learn more biomedcentral.com/submissions

